



# Phase-transition behavior and piezoelectric properties of lead-free $(\text{Ba}_{0.95}\text{Ca}_{0.05})(\text{Ti}_{1-x}\text{Zr}_x)\text{O}_3$ ceramics

Su-Wei Zhang, Hailong Zhang\*, Bo-Ping Zhang, Sui Yang

School of Materials Science and Engineering, University of Science and Technology Beijing, Xueyuan Road 30, Beijing 100083, China

## ARTICLE INFO

### Article history:

Received 13 May 2010

Received in revised form 17 June 2010

Accepted 24 June 2010

Available online 3 July 2010

### Keywords:

Ceramics

Ferroelectrics

Sintering

Phase transitions

Piezoelectricity

X-ray diffraction

## ABSTRACT

We report the enhancement of piezoelectric properties of  $(\text{Ba}_{0.95}\text{Ca}_{0.05})(\text{Ti}_{1-x}\text{Zr}_x)\text{O}_3$  (BCTZx) ceramics by optimizing Zr content in the range of  $0 \leq x \leq 15$  at.%. The BCTZx were synthesized by the solid-state reaction method and sintered at  $1350^\circ\text{C}$  in a reducing atmosphere of  $p\text{O}_2 = 5 \times 10^2$  Pa, for potential co-firing with base metal electrodes (BMEs). The BCTZx ceramics were characterized by an orthorhombic to pseudocubic polymorphic phase transition (PPT) at  $5 \leq x \leq 7$  at.%, based on X-ray diffraction patterns. The orthorhombic to pseudocubic phase-transition temperature  $T_1$  was shifted to  $36^\circ\text{C}$  near room temperature for Zr content of  $x = 4$  at.%. The piezoelectric constant  $d_{33}$ , electromechanical coupling coefficient  $k_p$ , and dielectric constant  $\epsilon_r$  were optimized to 338 pC/N, 36%, and 2070, respectively. The results indicate that optimizing Zr content is an effective way to enhance the piezoelectric properties of  $(\text{Ba,Ca})(\text{Ti,Zr})\text{O}_3$  ceramics, which are promising as a lead-free piezoelectric candidate.

© 2010 Elsevier B.V. All rights reserved.

## 1. Introduction

Environmental concern is calling for lead-free materials to substitute for widely used  $\text{Pb}(\text{Zr,Ti})\text{O}_3$  (PZT) ceramics. Niobate ceramics have become popular since Saito et al. [1] obtain a high  $d_{33}$  of 416 pC/N in textured  $(\text{K,Na})\text{NbO}_3$  (KNN)-based ceramics. Krauss et al. [2] also report good piezoelectric properties in  $(\text{Bi}_{0.5}\text{Na}_{0.5})\text{TiO}_3$  by forming a solid solution with  $\text{SrTiO}_3$ .  $\text{BaTiO}_3$  is a famous material that has been historically used in the field of piezoceramics [3] before the discovery of PZT. Nowadays  $\text{BaTiO}_3$  is mainly used as a dielectric but not a piezoelectric material, largely owing to the relatively lower piezoelectric properties compared with PZT. For the past several decades  $\text{BaTiO}_3$  ceramics have been showing a  $d_{33}$  level of only 190 pC/N [4]. Recently, surprisingly high  $d_{33}$  values of 350 pC/N [5], 419 pC/N [3], and 460 pC/N [6] are reported for  $\text{BaTiO}_3$  ceramics prepared by microwave sintering, ordinary sintering, and two-step sintering, respectively. Liu and Ren [7] even report a  $d_{33}$  as high as 620 pC/N in  $\text{BaTiO}_3$ -based ceramics by optimizing the composition to a tricritical triple point. The findings demonstrate that  $\text{BaTiO}_3$ -based ceramics possess a high possibility of replacing lead-containing PZT materials.

The  $(\text{Ca,Zr})$ -co-doped  $(\text{Ba,Ca})(\text{Ti,Zr})\text{O}_3$  ceramics are usually applied to produce the high-permittivity dielectrics of Y5V serials [8]. The  $(\text{Ba,Ca})(\text{Ti,Zr})\text{O}_3$  have been co-fired with Ni electrodes

in reducing atmospheres to produce multilayer ceramic capacitors (MLCCs) with base metal electrodes (BMEs) for a long time [9,10]. The  $(\text{Ca,Zr})$  co-doping plays a critical role in maintaining the electrical properties of  $\text{BaTiO}_3$  ceramics when sintered in a reducing atmosphere [8]. Our previous work [11] shows that a protective atmosphere of  $p\text{O}_2 = 5 \times 10^2$  Pa has a negligible effect on the phase structure, microstructure, and piezoelectric properties of  $(\text{Ba}_{0.95}\text{Ca}_{0.05})(\text{Ti}_{0.88}\text{Zr}_{0.12})\text{O}_3$  ceramics. A  $d_{33}$  of 200 pC/N is obtained for the composition of  $(\text{Ba}_{0.95}\text{Ca}_{0.05})(\text{Ti}_{0.88}\text{Zr}_{0.12})\text{O}_3$  by optimizing sintering temperature at  $1350^\circ\text{C}$  [11]. Thus the  $(\text{Ba,Ca})(\text{Ti,Zr})\text{O}_3$  ceramics show potential piezoelectric applications for co-firing with BMEs. The piezoelectric properties of  $(\text{Ba}_{0.95}\text{Ca}_{0.05})(\text{Ti}_{0.88}\text{Zr}_{0.12})\text{O}_3$  ceramics could be further enhanced by optimizing the content of dopants provided that there is a morphotropic phase boundary (MPB) or a polymorphic phase transition (PPT) associated with dopant content. Nanakorn et al. [12] recently address the dielectric and ferroelectric properties of  $\text{Ba}(\text{Ti}_{1-x}\text{Zr}_x)\text{O}_3$  ceramics by optimizing Zr content, but the piezoelectric properties are not reported.

In this study,  $(\text{Ba}_{0.95}\text{Ca}_{0.05})(\text{Ti}_{1-x}\text{Zr}_x)\text{O}_3$  ( $0 \leq x \leq 15$  at.%) are selected as lead-free compositions to investigate the compositional dependence of structure and electrical properties on Zr content. The enhancement of piezoelectric properties by optimizing Zr content in the  $(\text{Ba}_{0.95}\text{Ca}_{0.05})(\text{Ti}_{1-x}\text{Zr}_x)\text{O}_3$  ceramics is demonstrated.

## 2. Experimental details

Analytical-grade  $\text{BaCO}_3$ ,  $\text{CaCO}_3$ ,  $\text{TiO}_2$ , and  $\text{ZrO}_2$  powders (99.9%, Xilong Chemical Reagent, China) were used as raw materials. The powders were weighed according

\* Corresponding author. Tel.: +86 10 62332258; fax: +86 10 62332336.  
E-mail address: [hlzhang@ustb.edu.cn](mailto:hlzhang@ustb.edu.cn) (H. Zhang).

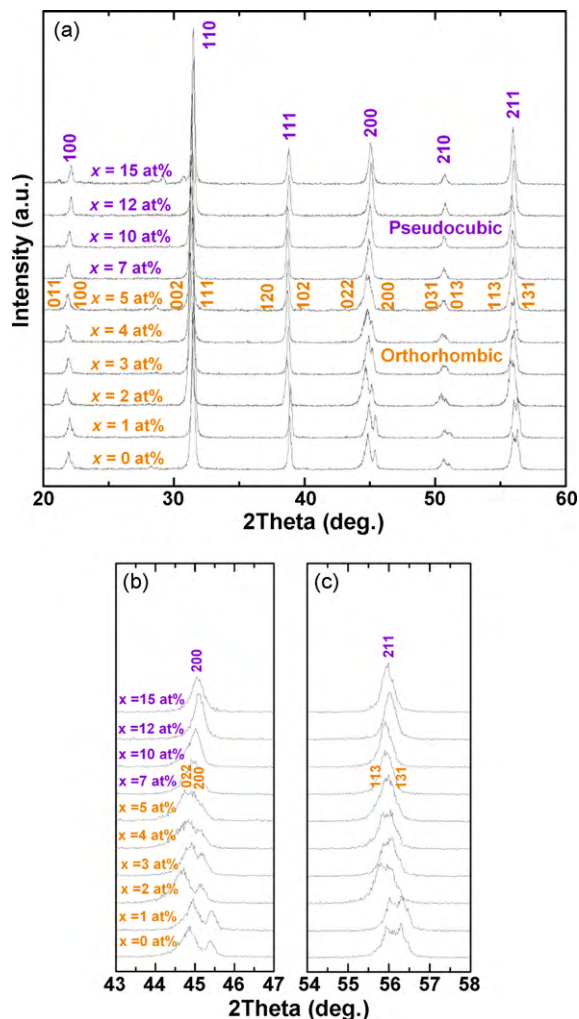


Fig. 1. X-ray diffraction patterns of the BCTZ<sub>x</sub> ( $0 \leq x \leq 15$  at.%) ceramics sintered at 1350 °C for 2 h in industrial N<sub>2</sub> gas.

to the chemical formula  $(\text{Ba}_{0.95}\text{Ca}_{0.05})(\text{Ti}_{1-x}\text{Zr}_x)\text{O}_3$  ( $0 \leq x \leq 15$  at.%), abbreviated as BCTZ<sub>x</sub>, and then ball mixed with ZrO<sub>2</sub> balls for 4 h using ethanol as the medium. The slurry was dried and then calcined at 1200 °C for 6 h in air. The calcined powders were mixed with a polyvinyl alcohol (PVA) binder solution and compacted into disk samples under 200 MPa. After burning out the binder at 700 °C for 30 min, the samples were sintered at 1350 °C for 2 h in an industrial N<sub>2</sub> gas (oxygen content: 0.5 vol.%) [11]. The chamber pressure was maintained at the atmospheric pressure of  $1.01 \times 10^5$  Pa, thus giving an oxygen partial pressure of  $5 \times 10^2$  Pa. Silver pastes were fired at 520 °C for 30 min on both sides of the sintered disk samples as electrodes for electrical measurements. The samples were poled at room temperature in a silicone oil bath under a dc field of  $\sim 3.0$  kV/mm for 20 min.

The crystalline structure was analyzed by X-ray diffraction (XRD) using a Cu K $\alpha$  radiation ( $\lambda = 1.5416$  Å) filtered through a Ni foil (Rigaku, RAD-B system, Japan). The sintered samples were polished and thermally etched at 1210–1260 °C for 30 min to inspect the microstructure using a scanning electron microscope (SEM, JSM-6460, Japan). The piezoelectric constant was measured 24 h after poling using a quasi-static piezoelectric  $d_{33}$  testing meter (ZJ-3A, Institute of Acoustics, China). The dielectric properties were measured from  $-20$  to 180 °C using an Agilent precision impedance analyzer (4294A, Hewlett-Packard, USA). The room-temperature dielectric constant was measured using an automatic component analyzer (TH2828S, Tonghui Electronics, China). Ferroelectric hysteresis loops were measured at room temperature using a ferroelectric tester (RT6000HVA, Radiant Technologies Inc., USA).

### 3. Results and discussion

Fig. 1(a) shows the XRD patterns of the BCTZ<sub>x</sub> ceramics sintered at 1350 °C for 2 h in the industrial N<sub>2</sub> gas. All the compositions exhibited a pure perovskite structure and no trace of impurity

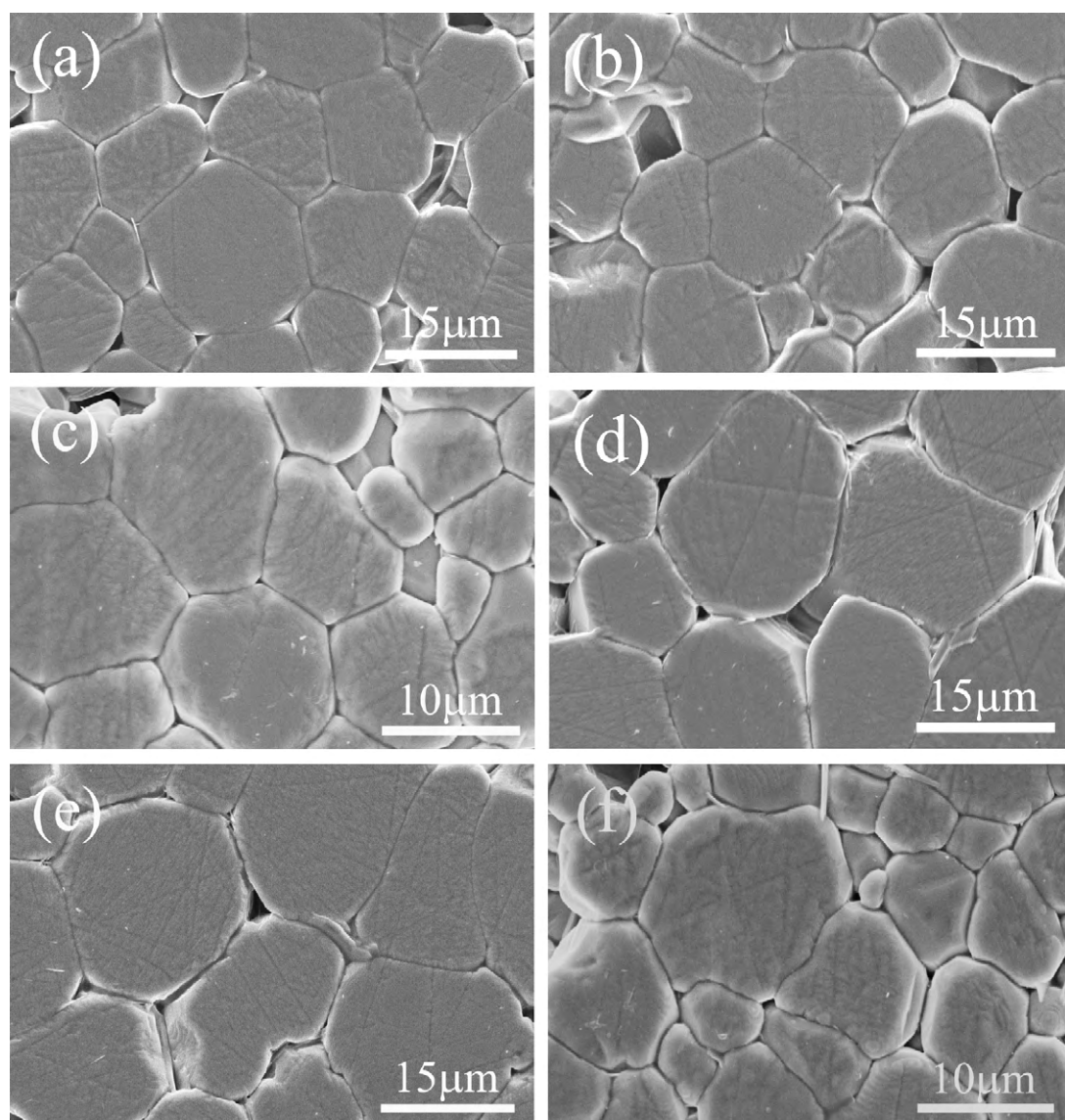
phase was observed, indicating that Ca<sup>2+</sup> and Zr<sup>4+</sup> have completely diffused into BaTiO<sub>3</sub> lattices to form solid solutions in the studied composition range. The BCTZ<sub>x</sub> ceramics were identified by two diffraction patterns of an orthorhombic symmetry (PDF card #81-2200) for  $0 \leq x \leq 5$  at.% and a pseudocubic symmetry (PDF card #31-0174) for  $7 \leq x \leq 15$  at.%. The orthorhombic to pseudocubic phase transition occurred at a phase boundary of  $5 \leq x \leq 7$  at.% at room temperature. The phase transition is caused by the distortion of crystal lattices induced by Ca<sup>2+</sup> ( $r = 0.99$  Å) occupying Ba<sup>2+</sup> sites (1.34 Å) and Zr<sup>4+</sup> (0.79 Å) occupying Ti<sup>4+</sup> (0.68 Å) sites. Fig. 1(b) shows the enlarged reflection lines in the  $2\theta$  range of 43–47°. With increasing Zr content from 0 to 5 at.% the diffraction peaks shifted to lower diffraction angles, since the substitution of Ti<sup>4+</sup> by larger Zr<sup>4+</sup> would expand the crystals of BCTZ<sub>x</sub>. This is the same case for the reflection lines in the  $2\theta$  range of 54–58° in Fig. 1(c).

Fig. 2 shows the SEM observations of the BCTZ<sub>x</sub> ceramics sintered at 1350 °C for 2 h in the industrial N<sub>2</sub> gas. With increasing Zr content the average grain size increased from  $\sim 9$  μm ( $x = 0$ ) to the maximum value of  $\sim 14$  μm ( $x = 5$  at.%), before gradually decreasing to  $\sim 6.5$  μm ( $x = 15$  at.%, not shown). This result shows the effect of Zr content on the microstructure evolution of the BCTZ<sub>x</sub> ceramics. Ramam and Lopez [13] have suggested that Ba doping increases the grain size of PZT-based ceramics, while excess Ba addition restrains the grain growth.

Fig. 3 shows the variations of dielectric constant and dielectric loss with temperature from  $-20$  to 180 °C for the poled BCTZ<sub>x</sub> samples, measured at 1 kHz. In the investigated temperature range, the BCTZ<sub>x</sub> ceramics ( $x \leq 12$  at.%) exhibited two phase-transition temperatures of Curie temperature  $T_c > 50$  °C and  $T_1$  near room temperature. The  $T_1$  was determined from the peaks in the  $\epsilon_r$ - $T$  curves shown in the inset to Fig. 3(a). Furthermore, Fig. 3(b) clearly describes the abrupt changes in dielectric loss  $\tan \delta$  at  $T_1$  and  $T_c$ , respectively, which are in accordance with the observations in Fig. 3(a). For pure BaTiO<sub>3</sub> ceramics the  $T_c$  and  $T_1$  are 120 and 5 °C, respectively [14]. The  $T_c$  of the BCTZ<sub>x</sub> ceramics was found to monotonously decrease towards lower temperatures with increasing  $x$ , which is consistent with the results reported for Ba(Ti<sub>1-x</sub>Zr<sub>x</sub>)O<sub>3</sub> ceramics [12] and Ba(Ti<sub>1-x</sub>Zr<sub>x</sub>)O<sub>3</sub> single crystals [15]. The BCTZ<sub>x</sub> ceramics at higher Zr contents showed broader dielectric constant-temperature ( $\epsilon_r$ - $T$ ) peaks at the vicinity of  $T_c$ , presenting some characteristics of diffuse ferroelectric phase transition [16].

As shown in Fig. 3, the sample with  $x = 0$  had a  $T_1$  of  $-5$  °C. The  $T_1$  gradually shifted to higher temperatures above room temperature with increasing  $x$  from 4 to 7 at.%. Further increasing  $x$  from 7 to 12 at.% caused  $T_1$  to shift to below room temperature again. When  $x = 15$  at.% the two phase transitions of  $T_1$  and  $T_c$  merged together and only one broad peak was observed at  $T_m$ , as shown in Fig. 3(a). At the same time, the dielectric loss showed no  $\tan \delta$ - $T$  peaks in the investigated temperature range due to the merging of  $T_1$  and  $T_c$ , as shown in Fig. 3(b). The result is in accordance with the Ba(Ti<sub>1-x</sub>Zr<sub>x</sub>)O<sub>3</sub> ( $0 \leq x \leq 30$  at.%) system [17]. This is the well-known pinching effect for the three phase transitions of pure BaTiO<sub>3</sub> when Ti<sup>4+</sup> is substituted with Zr<sup>4+</sup> [18]. The findings clearly demonstrate that the orthorhombic to pseudocubic phase transition observed in Fig. 1 is associated with a PPT behavior [19,20], but not a MPB behavior that is featuring a temperature stability of phase-transition composition. The MPB can be typically observed in Pb(Zr<sub>1-x</sub>Ti<sub>x</sub>)O<sub>3</sub> near the composition of Zr/Ti = 52/48 [18].

Special attention is paid to the  $(\text{Ba}_{0.95}\text{Ca}_{0.05})(\text{Ti}_{1-x}\text{Zr}_x)\text{O}_3$  compositions having a phase-transition temperature close to room temperature because the dielectric and piezoelectric properties were evaluated under ambient conditions in the present study. Released literature [20–22] reveals that shifting polymorphic phase-transition temperature downward to near room temper-



**Fig. 2.** SEM images of the BCTZ $x$  ceramics sintered at 1350 °C for 2 h in industrial N<sub>2</sub> gas with various Zr contents: (a) 0 at.%, (b) 3 at.%, (c) 4 at.%, (d) 5 at.%, (e) 7 at.%, and (f) 10 at.%.

ature greatly enhances piezoelectric properties of KNN-based ceramics. For the investigated BCTZ $x$  ceramics two compositions had a  $T_1$  close to room temperature, i.e.,  $\sim 36$  °C for  $x=4$  at.% and  $\sim 13$  °C for  $x=12$  at.%. It is noted that the PPT composition  $x=7$  at.% had a  $T_1$  of  $\sim 50$  °C, which is farther away from room temperature compared with  $x=4$  at.%. Although the  $T_1$  for another PPT composition of  $x=5$  at.% was not given this value should be in between 36 and 50 °C deduced reasonably from the variation tendency in Fig. 3, and is also farther away from room temperature compared with  $x=4$  at.%. It is generally accepted that a PPT composition determined at room temperature should also have a  $T_1$  near room temperature [20]. One could ascribe the above inconsistency to the reducing atmosphere of N<sub>2</sub> used in this study. Nevertheless, previous investigations have shown that the sintering atmosphere of N<sub>2</sub> has no substantial effect on the transition temperatures  $T_1$  or  $T_c$  of (Ba<sub>0.95</sub>Ca<sub>0.05</sub>)(Ti<sub>0.88</sub>Zr<sub>0.12</sub>)O<sub>3</sub> ceramics [11]. The interpretation to this inconsistency still remains open.

Fig. 4 shows the dielectric constant  $\epsilon_r$  and dielectric loss  $\tan \delta$  as functions of Zr content for the BCTZ $x$  ceramics. With increasing Zr content the  $\epsilon_r$  values first increased to a peaked value of 2070 at  $x=4$  at.% and then decreased slightly to 1478 at  $x=7$  at.%, before

increasing sharply to the maximum value of 2838 at  $x=15$  at.%. In the range of  $0 \leq x \leq 15$  at.%, the  $\epsilon_r$  values totally increased with increasing Zr content. Generally speaking, the pseudocubic-structured BCTZ $x$  ceramics exhibited higher dielectric constants than the orthorhombic-structured ones.

It is well known that dielectric constant abruptly increases at a phase-transition point. When the phase-transition point is close to room temperature, the dielectric constant measured at room temperature will be greatly increased. In this study, the peaked  $\epsilon_r$  at  $x=4$  at.% is in agreement with the fact that the  $T_1$  of 36 °C was close to room temperature. The  $T_1$  of 13 °C close to room temperature also increased greatly the  $\epsilon_r$  value at  $x=12$  at.%. Since the  $T_c$  was shifted close to room temperature the sample of  $x=15$  at.% had the highest  $\epsilon_r$  value, as shown in Fig. 4. The  $\tan \delta$  of the BCTZ $x$  ceramics also tended to increase with increasing  $x$  in the studied range and the maximum value was  $<0.036$ .

Fig. 5 shows the piezoelectric constant  $d_{33}$  and planar electromechanical coupling coefficient  $k_p$  as functions of Zr content for the BCTZ $x$  ceramics. There was a strong composition dependence of the piezoelectric properties. The highest piezoelectric properties were obtained at  $x=4$  at.%, yielding a  $d_{33}$  of 338 pC/N and

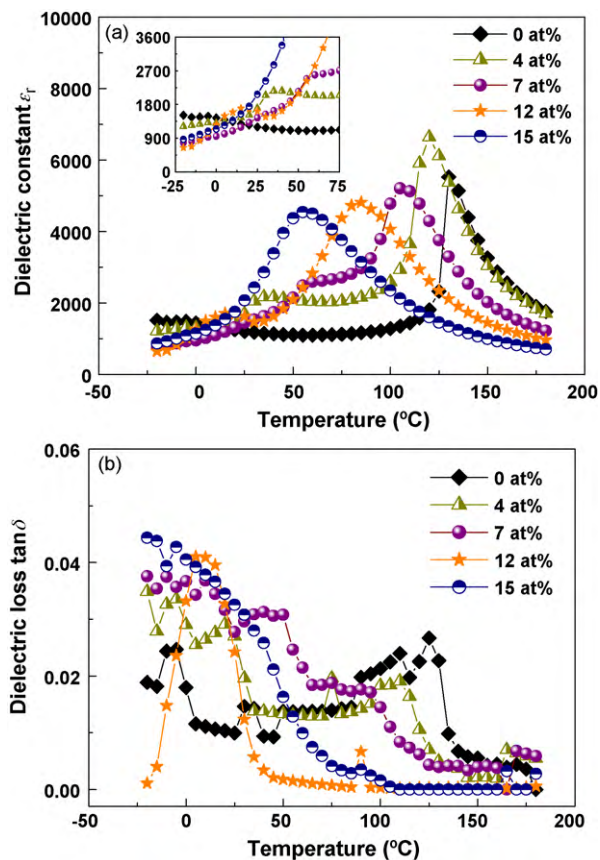


Fig. 3. Temperature dependences of (a) dielectric constant and (b) dielectric loss for the BCTZ $x$  ( $0 \leq x \leq 15$  at.%) ceramics sintered at 1350 °C for 2 h in industrial N $_2$  gas. Inset in (a) shows the enlarged  $\epsilon_r$ - $T$  curves in the temperature range of -25 to 75 °C.

a  $k_p$  of 36%. The  $d_{33}$  and  $k_p$  values were significantly enhanced by optimizing Zr content compared with previously reported (Ba $_{0.95}$ Ca $_{0.05}$ )(Ti $_{0.88}$ Zr $_{0.12}$ )O $_3$  ceramics [11]. The BCTZ $x$  ceramics also exhibited piezoelectric properties comparable to some lead-based ceramics.

As shown in Fig. 5, the  $d_{33}$  value was peaked at  $x=4$  at.% for the BCTZ $x$  samples. This result is supported by the finding that the phase-transition temperature  $T_1$  for  $x=4$  at.% was 36 °C, close to room temperature. The  $x=12$  at.% with  $T_1=13$  °C close to room temperature also had a peaked  $d_{33}$  value. It is revealed that shifting

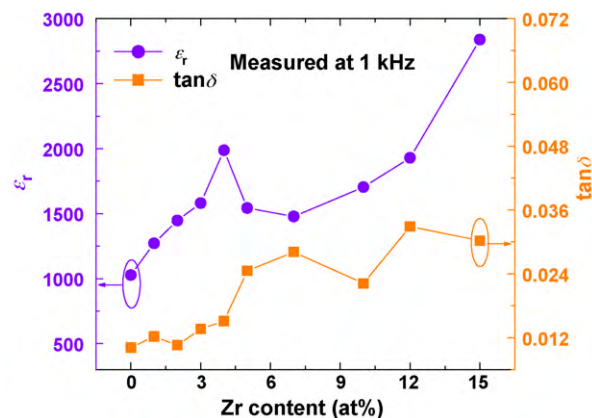


Fig. 4. Zr content dependences of dielectric constant and dielectric loss for the BCTZ $x$  ( $0 \leq x \leq 15$  at.%) ceramics sintered at 1350 °C for 2 h in industrial N $_2$  gas.

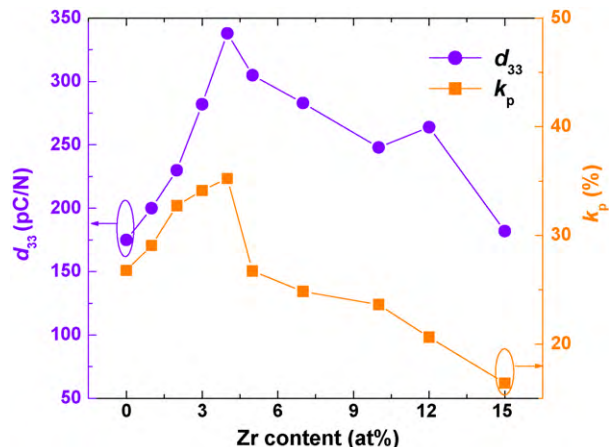


Fig. 5. Piezoelectric constant and electromechanical coupling coefficient as functions of Zr content for the BCTZ $x$  ( $0 \leq x \leq 15$  at.%) ceramics sintered at 1350 °C for 2 h in industrial N $_2$  gas.

transition temperature downward to near room temperature can greatly enhance the piezoelectric properties of KNN-based piezoceramics [22]. For example, Zhang et al. [21] significantly enhance the piezoelectric constant  $d_{33}$  from 127 pC/N for KNN ceramics to 265 pC/N for 0.948KNN–0.052LiSbO $_3$  ceramics by shifting the orthorhombic to tetragonal phase-transition temperature from 195 °C for KNN to 35 °C for 0.948KNN–0.052LiSbO $_3$  with doping LiSbO $_3$ . However, it is noted that the two compositions of  $x=4$  and 12 at.% were not in the range of  $5 \leq x \leq 7$  at.% that was identified for PPT in the present study. This implies that the proximity of phase-transition temperature to room temperature plays more important roles in enhancing piezoelectric properties of the BCTZ $x$  ceramics.

Fig. 6 shows the hysteresis loops ( $P$  versus  $E$ ) of the BCTZ $x$  ceramics with various Zr contents. The Zr content was found to have an obvious effect on the ferroelectric properties of the (Ba $_{0.95}$ Ca $_{0.05}$ )(Ti $_{1-x}$ Zr $_x$ )O $_3$  ceramics. As shown in the inset to Fig. 6, the remnant polarization  $P_r$  decreased gradually from 15.12 to 5.27  $\mu\text{C}/\text{cm}^2$  with increasing  $x$  from 0 to 15 at.%. The result suggests that the orthorhombic-structured BCTZ $x$  ceramics possess higher  $P_r$  values than the pseudocubic-structured ones, which is consistent with reported Ba(Ti $_{1-x}$ Zr $_x$ )O $_3$  single crystals [15]. Further explanation is the summation of spontaneous polarization directions for an orthorhombic phase is more than that for a pseudocubic phase [21].

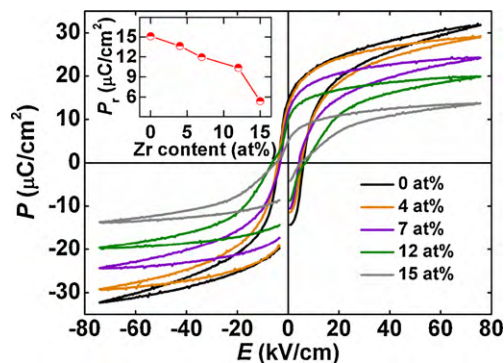


Fig. 6.  $P$ - $E$  hysteresis loops measured for the BCTZ $x$  ( $0 \leq x \leq 15$  at.%) ceramics sintered at 1350 °C for 2 h in industrial N $_2$  gas. Inset represents the variation of remnant polarization  $P_r$  as a function of Zr content.

#### 4. Conclusions

The  $(\text{Ba}_{0.95}\text{Ca}_{0.05})(\text{Ti}_{1-x}\text{Zr}_x)\text{O}_3$  ( $0 \leq x \leq 15$  at.%) piezoceramics were synthesized by the solid-state reaction method and sintered at  $1350^\circ\text{C}$  for 2 h in the industrial  $\text{N}_2$  gas. The PPT of orthorhombic to pseudocubic for the BCTZx ceramics was identified at  $5 \leq x \leq 7$  at.% through XRD patterns. Excellent electrical properties of  $d_{33} = 338$  pC/N,  $k_p = 36\%$ , and  $\varepsilon_r = 2070$  were obtained at  $x = 4$  at.% near the PPT compositions. The results indicate that appropriate Zr addition ( $4 \leq x \leq 7$  at.%) can significantly improve the piezoelectric properties of  $(\text{Ba}_{0.95}\text{Ca}_{0.05})(\text{Ti}_{1-x}\text{Zr}_x)\text{O}_3$  ceramics. The present study demonstrates that  $(\text{Ba,Ca})(\text{Ti,Zr})\text{O}_3$  ceramics are a promising candidate for lead-free piezoceramics.

#### Acknowledgements

This work was financially supported by the High-Tech 863 Program of China (Grant No. 2006AA03Z436) and the National Key Technology R&D Program of China (Grant No. 2008BAB32B11).

#### References

- [1] Y. Saito, H. Takao, T. Tani, T. Nonoyama, K. Takatori, T. Homma, T. Nagaya, M. Nakamura, *Nature* 432 (2004) 84–87.
- [2] W. Krauss, D. Schutz, F.A. Mautner, A. Feteira, K. Reichmann, *J. Eur. Ceram. Soc.* 30 (2010) 1827–1832.
- [3] S.F. Shao, J.L. Zhang, Z. Zhang, P. Zheng, M.L. Zhao, J.C. Li, C.L. Wang, *J. Phys. D: Appl. Phys.* 41 (2008), 125408 (6pp).
- [4] R. Bechmann, *J. Acoust. Soc. Am.* 28 (1956) 347–350.
- [5] H. Takahashi, Y. Numamoto, J. Tani, S. Tsurekawa, *Jpn. J. Appl. Phys.* 45 (2006) 7405–7408.
- [6] T. Karaki, K. Yan, T. Miyamoto, M. Adachi, *Jpn. J. Appl. Phys.* 46 (2007) L97–L98.
- [7] W.F. Liu, X.B. Ren, *Phys. Rev. Lett.* 103 (2009), 257602 (4pp).
- [8] D.F.K. Hennings, H. Schreinemacher, *J. Eur. Ceram. Soc.* 15 (1995) 795–800.
- [9] H. Kishi, Y. Mizuno, H. Chazono, *Jpn. J. Appl. Phys.* 42 (2003) 1–15.
- [10] T.A. Jain, K.Z. Fung, J. Chan, *J. Alloys Compd.* 468 (2009) 370–374.
- [11] S.W. Zhang, H.L. Zhang, B.P. Zhang, G.L. Zhao, *J. Eur. Ceram. Soc.* 29 (2009) 3235–3242.
- [12] N. Nanakorn, P. Jalupoom, N. Vaneesorn, A. Thanaboonsombut, *Ceram. Int.* 34 (2008) 779–782.
- [13] K. Ramam, M. Lopez, *J. Eur. Ceram. Soc.* 27 (2007) 3141–3147.
- [14] M. Budimir, D. Damjanovic, N. Setter, *J. Appl. Phys.* 94 (2008) 6753–6761.
- [15] Z. Yu, R.Y. Guo, A.S. Bhalla, *Appl. Phys. Lett.* 77 (2000) 1535–1537.
- [16] X.G. Tang, K.H. Chew, H.L.W. Chan, *Acta Mater.* 52 (2004) 5177–5183.
- [17] Z. Yu, C. Ang, R. Guo, A.S. Bhalla, *J. Appl. Phys.* 92 (2002) 1489–1493.
- [18] B. Jaffe, W.R. Cook, H. Jaffe, *Piezoelectric Ceramics*, Academic Press, London, New York, 1971.
- [19] D.W. Baker, P.A. Thomas, N. Zhang, A.M. Glazer, *Appl. Phys. Lett.* 95 (2009), 091903 (3pp).
- [20] Y.J. Dai, X.W. Zhang, K.P. Chen, *Appl. Phys. Lett.* 94 (2009), 042905 (3pp).
- [21] S.J. Zhang, R. Xia, T.R. Shrout, G.Z. Zang, J.F. Wang, *J. Appl. Phys.* 100 (2006), 104108 (6pp).
- [22] E. Hollenstein, D. Damjanovic, N. Setter, *J. Eur. Ceram. Soc.* 27 (2007) 4093–4097.